ELSEVIER

Research report

Functional magnetic resonance imaging of brain activity in the visual oddball task

Babak A. Ardekani[a,d,*], Steven J. Choi[g], Gholam-Ali Hossein-Zadeh[a], Bernice Porjesz[c], Jody L. Tanabe[b], Kelvin O. Lim[g], Robert Bilder[a], Joseph A. Helpern[a,d,e,f], Henri Begleiter[c]

[a]*Center for Advanced Brain Imaging, Nathan Kline Institute for Psychiatric Research, 140 Old Orangeburg Road, Orangeburg, NY 10962, USA*
[b]*Department of Radiology, University of Colorado Health Sciences Center, Denver, CO, USA*
[c]*Department of Psychiatry, State University of New York Health Science Center at Brooklyn, Brooklyn, NY, USA*
[d]*Department of Psychiatry, New York University School of Medicine, New York, NY, USA*
[e]*Department of Radiology, New York University School of Medicine, New York, NY, USA*
[f]*Departments of Physiology and Neuroscience, New York University School of Medicine, New York, NY, USA*
[g]*Department of Psychiatry, University of Minnesota, Minneapolis, MN, USA*

Abstract

Abnormalities in the P300 ERP, elicited by the oddball task and measured using EEG, have been found in a number of central nervous system disorders including schizophrenia, Alzheimer's disease, and alcohol dependence. While electrophysiological studies provide high temporal resolution, localizing the P300 deficit has been particularly difficult because the measurements are collected from the scalp. Knowing which brain regions are involved in this process would elucidate the behavioral correlates of P300. The aim of this study was to determine the brain regions involved in a visual oddball task using fMRI. In this study, functional and high-resolution anatomical MR images were collected from seven normal volunteers. The data were analyzed using a randomization-based statistical method that accounts for multiple comparisons, requires no assumptions about the noise structure of the data, and does not require spatial or temporal smoothing. Activations were detected ($P<0.01$) bilaterally in the supramarginal gyrus (SMG; BA 40), superior parietal lobule (BA 7), the posterior cingulate gyrus, thalamus, inferior occipitotemporal cortex (BA 19/37), insula, dorsolateral prefrontal cortex (BA 9), anterior cingulate cortex (ACC), medial frontal gyrus (BA 6), premotor area, and cuneus (BA 17). Our results are consistent with previous studies that have observed activation in ACC and SMG. Activation of thalamus, insula, and the occipitotemporal cortex has been reported less consistently. The present study lends further support to the involvement of these structures in visual target detection.
© 2002 Elsevier Science B.V. All rights reserved.

1. Introduction

The P300 event-related potential (ERP) is observed in electroencephalography (EEG) when subjects are instructed to detect infrequently occurring *target* sensory stimuli imbedded in an otherwise repetitive train of frequent *standard* stimuli. This stimulation paradigm is known as the *oddball task* (see Section 2 for a more detailed description). The name P300 is due to the fact that the EEG potential is positive and is observed approximately 300 ms after the occurrence of the target stimuli. This phenomenon was first observed by Sutton et al. [32] and since then abnormalities in the P300 ERP have been found in a number of central nervous system disorders, including schizophrenia [13], Alzheimer's disease [15], and alcohol dependence [29]. While the underlying mechanism for the abnormal P300 ERP is not known, it is believed to be associated with impairments in arousal, attention, infor-

---

mation processing speed, and working memory requirements involved in the performance of the oddball task [28].

The ERP literature suggests that activity in the oddball task may involve multiple brain regions, including cortical, thalamic, and limbic regions [28]. However, given the 'inverse problem' of localizing neural generators from surface potentials, there are significant challenges in determining the precise regional contributions to the P300 by EEG alone [24]. To address this problem, several research groups have applied functional magnetic resonance imaging (fMRI) to localize the P300 sources [7,17,20,22,23,26,31,34]. fMRI offers a means for localization of brain activity that complements high temporal resolution recordings achievable with EEG. Two cortical regions that consistently activate, as reported in previous fMRI studies irrespective of the type of sensory stimuli (visual or auditory), are the bilateral supramarginal gyri (SMG; BA[1] 40); and the anterior cingulate cortex (ACC). However, the involvement of a number of other regions has been more ambiguous. For example, only half of the studies reported detecting thalamic activation during the performance of the oddball task [7,17,23,34]; insular cortex was reported to be activated in fewer than half of the previous studies [7,20,34]; and only one study reported activation of the cerebellum [7]. Another region that is believed to be involved in target detection is the dorsolateral prefrontal cortex (DLPFC). Although five of the previous fMRI studies of the oddball task reported activation of this area [7,17,22,31,34], there is disagreement over the laterality of the activation. Of these, two studies detected bilateral activation of the DLPFC [22,34], while the other three studies only reported activation of the right DLPFC [7,17,31]. Therefore, while the existing studies have contributed greatly to our understanding of the brain regions underlying performance of the oddball task, further studies are required to elucidate the role of subcortical structures as well as cortical regions other than SMG and ACC.

There are several factors that could explain the differences between findings reported in previous fMRI studies of the oddball task. Studies performed by different groups vary widely in the stimulation paradigm (e.g. type of sensory stimulus; frequency of rare events; number of trials), scanning parameters (e.g. slice thickness; repetition time; brain coverage), and statistical analysis method. For example, only two of the previous fMRI studies [7,17] have incorporated full-brain or near full-brain coverage to examine event-related brain activation associated with the oddball paradigm.

The number of target events is an important factor since a large number of target events may be necessary to detect regions with low signal-to-noise that may otherwise be labeled inactive. On the other hand, sufficient time be-

tween the target events should be allowed so that deviations from linearity assumptions inherent in most fMRI analysis techniques do not significantly diminish the sensitivity of the methods. As mentioned above, the choice of the activation detection algorithm is also an important consideration. Assumptions about the noise structure (e.g. Gaussian white noise with a Gaussian spatial autocorrelation structure) are necessary to obtain reliable results in some parametric activation detection methods [14]. These assumptions are not necessarily satisfied in fMRI. Therefore, if statistical inference about the location and degree of activation is to be made based on such assumptions, it may be necessary to apply heavy smoothing to bring the data into approximate compliance. Smoothing sacrifices the spatial resolution of fMRI that is important in functional brain mapping in general. The purpose of this study was to re-examine the brain regions involved in visual target detection, using near full-brain coverage and a novel non-parametric randomization-based statistical analysis method. The analysis method does not rely on any assumptions about the noise structure in the data, does not require smoothing (other than the unavoidable smoothing introduced by spatial normalization and inter-subject data fusion), and controls for multiple comparisons.

2. Materials and methods

2.1. Subjects

Seven healthy normal subjects with no history of psychiatric or neurological disorders were recruited for this study (ages 25–42; mean age 32; five females; two males). The Institutional Review Board (IRB) of the Nathan Kline Institute approved all procedures. Written informed consent was obtained from all participants.

2.2. Task

The task given to the subjects in this experiment is known as the 'classic visual oddball paradigm' in the EEG literature. In this task, a train of equally spaced visual stimuli is presented to the subjects. There are two types of stimuli: the standard stimuli, and the target stimuli. The standard events occur more frequently than the target events. The subjects are instructed to silently count the target stimuli and report the total number at the end of the experiment. In the present study, the standard visual stimulus (93.75% of trials) was an image consisting of the string of white characters 'OOOOO' on a dark background, while the target image (6.25% of trials) was the string of characters 'XXXXX'. Visual stimuli were delivered to the subject via a liquid crystal display (LCD) mounted on the MRI scanner's radio frequency (RF) head coil. The LCD display was connected to the video graphics array (VGA) output of a personal computer (PC) outside

---

[1]Brodmann Area.

the scanner room. A total of 1024 images were shown to the subjects (64 targets and 960 standards) in four experimental runs of 256. The inter-stimulus interval (ISI) was 1648 ms. Stimulus duration was approximately 500 ms. During the remaining time (~1148 ms) the screen was dark. There was a slight delay (less than 10 s) between experimental runs, which was required to reload the MRI scanner pulse sequence. The target events were distributed randomly amongst the four runs and 1024 trials, but it was ensured that there were at least eight frequent events between every pair of target events. The average inter-trial interval between successive target stimuli was approximately 26 s ranging from 14.8 to 56 s. The temporal structure of the train of stimuli, although randomly selected, was identical across all seven subjects.

2.3. Image acquisition

Images were acquired using a 1.5 T Siemens Vision MRI system (Siemens AG, Erlangen, Germany) located at the Center for Advanced Brain Imaging of the Nathan Kline Institute. A quadrature head coil was used for RF transmission and reception. The subjects were given earplugs and were positioned supine and comfortably in the magnet. Cushions were placed around the subject's head to reduce motion. Scanning began with a number of localizer scans used to orient the functional scans approximately perpendicular to the mid-sagittal plane and parallel to the line connecting the anterior and posterior commissures (AC–PC line). Blood oxygenation level-dependent (BOLD) functional scans were obtained using a T_2^*-weighted gradient echo single-shot echo-planar imaging (EPI) sequence with TR=1648 ms, TE=45 ms, Flip Angle=90°, and FOV=250×250 mm^2. A total of 1024 EPI volumes were acquired from each subject. Each volume covered nearly the entire cerebrum and the superior aspect of the cerebellum, consisting of 15 transverse slices of size 64×64 with a pixel size of approximately 3.91×3.91 mm^2 and a slice thickness of 6 mm with no gaps. The acquisition of each EPI volume was synchronized with the onset of a visual stimulus. The synchronization was achieved by triggering the MRI scanner using an external TTL pulse generated by the stimulus presentation PC. In addition to the EPI data, a high-resolution anatomical 3D T_1-weighted image volume was acquired from each subject using a magnetization-prepared rapid acquisition gradient echo (MP-RAGE) sequence. The scan parameters for this sequence were TR=11.6 ms, TE=4.9 ms, Flip Angle=8°, FOV=256×256×190 mm^3, with a matrix size of 256×256×190 volume elements (voxels), yielding a 1 mm^3 isotropic voxel size.

Two areas of the cerebrum were not covered by the EPI sequence in all subjects: the orbital frontal area and the anterior inferior temporal lobe. The orbital frontal area is difficult to image using EPI because of strong susceptibility artifacts. The anterior inferior temporal lobe was
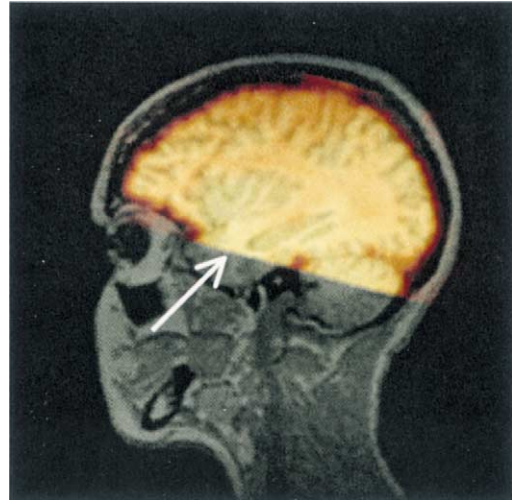
Fig. 1. Fusion of an EPI image (hot metal color) with an anatomical MP-RAGE image (gray scale) from one of the subjects in the study. The fusion was carried out after the images were spatially registered using the procedure outlined in Section 2.4. The arrow indicates the area of the temporal lobe that was not imaged by the EPI sequence for most subjects.

not imaged because of the inadequate number of slices possible to acquire within the limit set by the TR of the paradigm. Fig. 1 shows the fusion of an EPI image (hot metal color) with an anatomical MP-RAGE image (gray scale) from one of the subjects in the study. The fusion was carried out after the images were spatially registered using the procedure outlined in the following section. The arrow indicates the area of the temporal lobe that was not imaged by the EPI sequence for most subjects.

2.4. Image processing

The images were transferred to an 800 MHz Dell Precision Workstation 420 (Dell Computer Co., Round Rock, TX) running the Red Hat Linux 6.2 operating system (Red Hat Co., Durham, NC). The first four scans from each of the four experimental runs of 256 were discarded to ensure steady state magnetization, leaving a total of 1008 EPI volumes to be analyzed for each subject. Motion detection and correction was performed on the data using the motion correction module of the AFNI software package [9] (Medical College of Wisconsin, Milwaukee, WI). Accuracy of this motion correction method was validated in a separate study [1].

After motion correction, the 1008 EPI volumes were averaged. The intracranial region was segmented by thresholding the average image. The threshold was selected automatically by analyzing the average image histogram. It was selected to be the trough between the two main peaks of the histogram that correspond to the background noise and the brain voxels. Following this, a connected component analysis was performed that selects the largest four-connected component in the thresholded binary image

as the brain and removes all other small components. In addition, the largest four-connected component is made *simply connected* by filling any cavities within it. This method of brain detection is similar to that used by Belmonte and Yurgelun-Todd [3].

Following the definition of the brain mask, the brain voxels' time-series were centered to have zero mean. In addition, several 'trend' components were regressed out of each time-series. The trends were identified by principal component analysis (PCA) of the data from all brain voxels. The number of principal components that were identified and removed from the data sets varied from subject to subject. A heuristic method for identifying the number of components was used, namely that the component had to explain at least 3% of the total variation in the data *and* have a cross-correlation of less than 0.05 with the reference vector representing the stimulus presentation pattern. This heuristic procedure identified between two and six components depending on the subject under study. Our experience on data from the present study, as well as data from other experiments, shows that this method of detrending increases the sensitivity of analyses. The first PCs from different subjects are usually similar and show a pseudo-linear drift. The subsequent PCs vary to a greater extent between subjects. We have also observed that in many cases, the PCs that are removed correlate highly with the motion parameters determined independently by the motion detection algorithm. The first PCs that were identified and removed from four of our subjects are displayed in Fig. 2.

Following the preprocessing of the EPI data by motion correction and trend removal by PCA, the sagittal MP-RAGE images from each subject were spatially registered to the raw axial EPI volumes of the same subject. Since the
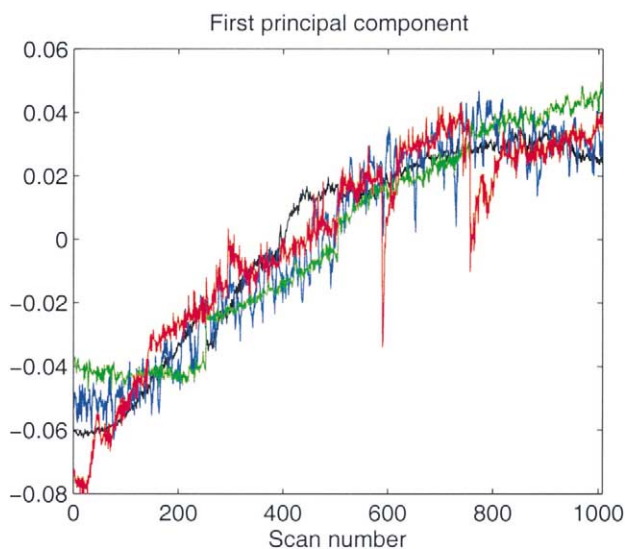
Fig. 2. The first principal components identified as trends using PCA and removed from the data in four subjects. In most subjects, the first PC had a pseudo-linear appearance as shown.

EPI and MP-RAGE volumes were scanned during the same session, the transformation required for the MP-RAGE to EPI registration was deduced from the header information contained in the Siemens Vision file format. The resulting axial MP-RAGE images were transformed into the Talairach–Tourneaux stereotactic atlas [33] using the AFNI software package. The same transformation was then applied to the EPI volumes to transform them into the Talairach–Tourneaux coordinates. The transformed EPI volumes were resampled to a voxel size of $3 \times 3 \times 3$ mm^3 and a matrix size of $54 \times 64 \times 50$. Finally, the spatially normalized and resampled EPI data from all seven subjects were fused by computing their *median*, resulting in a single EPI data set representing the entire group. We shall refer to this data set as the 'median data set'. The median is immune to outliers and avoids the situation where a strong region of activation in a single subject may be incorrectly attributed to the entire group.

2.5. Statistical analysis

Non-parametric randomization-based statistical methods were employed for detecting the activated brain regions. Such methods have been previously applied to the analysis of functional images by Blair and Karniski [4] and Holmes et al. [16]. These authors were mainly concerned with brain mapping experiments using positron emission tomography (PET). However, their methods may be adapted to fMRI with some modifications. Brammer et al. [5] applied permutation testing to the analysis of fMRI data. Their method required a small number of permutations, but only controlled for voxel-wise false positive rates and did not handle the multiple comparisons problem. For fMRI analysis, Belmonte and Yurgelum-Todd [3] devised an algorithm for an efficient implementation of the step-down test that had been originally described by Holmes et al. [16] for PET. This method has the advantage that it controls for image-wise false positive rate, thus, circumventing the multiple comparisons problem. Its implementation is publicly available as a plug-in module in the AFNI software package. In this method, the permutations are carried out by reshuffling the temporal sequence of observations. This type of resampling destroys the temporal autocorrelation in the data. As a result, it may exaggerate the sensitivity of the algorithm and increase the false alarm rate. Belmonte and Yurgelum-Todd [3] suggested that the results may be improved by removing the temporal autocorrelation in the observed time-series. Locascio et al. [21] dealt with this problem by modeling the temporal autocorrelation as an autoregressive moving average (ARMA) stochastic process. Recently, Bullmore et al. [6] suggested a method of resampling in the wavelet domain that preserves the temporal autocorrelation in time. For each permutation, the model reshuffles the wavelet coefficient and then takes the inverse wavelet transform. We have implemented this algorithm and have observed that

Table 1
Target detection rates and the significance levels of the global null hypothesis (omnibus) test

Subject ID	No. targets detected	Omnibus test P-value
203	64	0.001
502	60	0.002
702	64	0.001
703	64	0.001
101	65	0.001
302	55	0.062
103	64	0.001

when the length of the time-series becomes large (such as 1008 in this study), the wavelet transformations become exceedingly time consuming. In the method applied in our report, we randomize the times when the stimuli are applied instead of randomizing the sequence of observations (i.e. the fMRI volumes) in time. Thus, at each iteration the observed fMRI time series remains exactly the same and any temporal autocorrelation present in the data remains intact.

The EPI data from each subject were first analyzed separately before transformation into the Talairach–Tourneaux stereotactic space. For each subject, we tested the global null hypothesis, $H_0^{(G)}$ that there was no activation produced by our experimental paradigm anywhere in the brain. For each voxel n, a statistic was computed as follows:

$$s_n = \frac{\mathbf{x}_n \cdot \hat{\mathbf{r}}}{\sqrt{\mathbf{x}_n \cdot \mathbf{x}_n}} \tag{1}$$

This statistic is the cosine of the angle between the fMRI time-series vector $\mathbf{x}_n$ and a reference vector $\hat{\mathbf{r}}$ and, therefore, varies between -1 and 1. It is better known as the cross-correlation statistic in fMRI literature. Note that in Eq. (1), it is assumed that $\mathbf{x}_n$ and $\hat{\mathbf{r}}$ have zero-mean and $\hat{\mathbf{r}}$ is normalized. The reference vector models the changes in image intensity that we expect to observe from the experimental stimulation paradigm. In general, higher values of the test statistic defined by Eq. (1) provide evidence of the presence of activation. The reference vector $\hat{\mathbf{r}}$ was obtained by convolving a train of impulses representing the target events with the gamma hemodynamic impulse response function [18]:

$$h(t:\tau,\delta) = \begin{cases} e^{-t/\sqrt{\delta}\tau}\left(\dfrac{et}{\tau}\right)^{\sqrt{\tau/\delta}} & t > 0 \\ 0 & t < 0 \end{cases} \tag{2}$$

where the parameter $\tau = 4.7$ s marks the peak of the gamma impulse response function, and $\delta = 0.06$ is a dimensionless parameter that controls its shape. The mean of the resulting time-series was then removed and it was normalized to obtain $\hat{\mathbf{r}}$.

In the non-parametric randomization-based method for testing the global null hypothesis $H_0^{(G)}$, the entire data set was analyzed 1000 times, each time assuming a different set of non-coinciding times of occurrences for the target events or equivalently a different reference vector $\hat{\mathbf{r}}$. In only one of these analyses, $\hat{\mathbf{r}}$ represented the actual times of target events in the experiment. In the other 999 analyses, the target events were randomized and had no special relationship with the experimental paradigm. Note that in this method, the order of the scans in time was *not* altered and, therefore, any existing temporal correlation in the data remained intact. Randomization is only performed on times of occurrences of the target events. Because of the presence of temporal correlations in the fMRI data, if the scan times were randomized, the required data exchangeability condition could not be guaranteed. For each of the 1000 analyses, the maximal statistic $s_{max} = \max_n (s_n)$ was determined. The global null hypothesis $H_0^{(G)}$ was rejected at $P = 0.05$ level if the maximal statistic s_{max} obtained when using the actual non-randomized $\hat{\mathbf{r}}$ was in the top 5 percentile of the distribution of the maximal statistic in all 1000 analyses.

As mentioned in the previous section, the motion-corrected, detrended, and spatially normalized EPI images from all subjects were combined by taking their median. We carried out 1000 randomization analyses of the median data set, using the exact same procedure described in the preceding paragraph, to localize the activation within the brain. All voxels for which the test statistic s_n fell within the top 1 percentile of the empirically determined probability distribution function of the maximal test statistic were declared activated. We also implemented the *step-down* version of the above test as described in Ref. [16]. The step-down test is expected to increase the sensitivity of the detection technique. However, at least in the present data, we saw very little change compared to the results of the single-step test described above. It can be shown that both the single-step and the step-down tests effectively deal with the multiple comparisons problem [16]. Controlling for multiple comparisons means that if in reality no voxel is activated anywhere in the brain (i.e. the global null hypothesis $H_0^{(G)}$ is true), the probability that at least one voxel somewhere in the brain is (falsely) declared activated by the activation detection test is at most equal to α (in this case 0.01). Mathematically, this can be written as: $P(s_1 \cup s_2 \cup \cdots s_k > T) \leq \alpha$ where the symbol $\cup$ denotes the logical 'or' operation, k is the total number of brain voxels, and T is the threshold used for detecting activation in the statistic image $\{s_n: n = 1 \cdots k\}$. To show that the permutation test described above controls for multiple comparisons, we note that the probability that at least in some brain voxel the statistic s_n is greater than a given threshold T, is less than or equal to the probability that s_{max} is greater than T, that is:

$$P(s_1 \cup s_2 \cup \cdots s_k > T) \leq P(s_{max} > T) \tag{3}$$

Since we choose the threshold T such that $P(s_{max} > T) =$

α, then inequality (3) implies that $P(s_1 \cup s_2 \cup \cdots s_k > T) \le \alpha$, that is, the test controls for multiple comparisons.

3. Results

3.1. Target detection rates

Four of the seven subjects reported having seen the correct number of targets (64). One subject reported 65, and the other two subjects counted 55 and 60 target stimuli. The data are shown in Table 1.

3.2. Omnibus test of activation

Table 1 also shows the P-values obtained for each subject for the global null hypothesis test of no activation anywhere in the brain, $H_0^{(G)}$. The test was rejected in all but one subject who had an omnibus test P-value of 0.062 that was just above the significance level. It is interesting to note that the subject for whom the omnibus null hypothesis was not rejected reported having seen only 55 target events.

3.3. Localization of the activation

Activation was detected in several brain areas. Fig. 3 shows the activated regions superimposed on the MP-RAGE image of one of the subjects registered to the Talairach–Tourneaux stereotactic atlas. Activations were detected in the inferior parietal lobule (SMG) in BA 40 (Fig. 3a); superior parietal lobule (BA 7, Fig. 3b); the posterior cingulate gyrus (BA 23, Fig. 3c); thalamus (Fig. 3d); inferior occipitotemporal cortex (BA 19/37, Fig. 3e); insula (Fig. 3f); middle frontal gyrus (DLPFC, BA 9, Fig. 3g); ACC (BA 24, Fig. 3h); medial frontal gyrus (BA 6, Fig. 3h); premotor area (BA 6, Fig. 3i); and cuneus (BA 17, Fig. 3j). All activations were bilateral. The average (across voxels and target events) of the evoked stimulus responses in the median data set for the left and right DLPFC and the ACC are shown in Fig. 4.

4. Discussion

As in the majority of the previous fMRI studies reported for this paradigm, we found activation in the bilateral SMG (Fig. 3a) and ACC (Fig. 3h). We also detected bilateral thalamic activation (Fig. 3d). Only half of the previous studies had reported activation of the thalamus during the performance of the oddball task [7,17,23,34]. In these studies, Kiehl and Liddle [17] and Menon et al. [23] used auditory stimuli, Clark et al. [7] visual stimulation, while Yoshiura et al. [34] performed both visual and auditory experiments. Our findings provide additional evidence that the thalamus is involved in target detection. Furthermore,

thalamic activation appears to be modality-independent. The results are also consistent with the findings from deep electrode studies, which have suggested P300 generation in the thalamus during target detection [30].

The DLPFC plays a key role in working memory. We found bilateral activation of the DLPFC (Fig. 3g). Several previous studies also detected activation of the DLPFC during the oddball task [7,17,22,31,34]. However, the previous studies have been divided over the question of whether the activation is bilateral or only the right side of the brain is engaged. Our finding supports the bilateral activation hypothesis. A theory that reconciles the differences between the studies is that while the activation of the DLPFC is bilateral, it may be stronger, or to a greater extent, on the right side of the brain and, hence, easier to detect. For the data analyzed in this study, the number of activated voxels on the right DLPFC (50) was substantially greater than those on the left DLPFC (20). The average evoked BOLD responses in the two regions are shown in Fig. 4. A paired samples t-test between the two curves did not show a statistically significant difference between the BOLD responses of the two regions ($P = 0.667$). These results suggest that although the extent of activation is different between the two regions, the level of BOLD signal changes are comparable.

The bilateral activation of the insular cortex found in the present (Fig. 3f) study lends additional support to the insula activation found in a subset of the previous studies of the oddball task [7,20,34]. The activation appears to be modality-independent. Insula is known to be involved in somatosensory, language, and other non-cognitive functions [2]. However, its role in cognition is not well established. It has been shown that the insula may be involved in verbal working memory [27] and selective attention [8], which would be consistent with the functions tapped by the design of this study.

Activation of the posterior cingulate cortex (PCC) has been controversial in previous studies of the P300. Kiehl and Liddle [17] and McCarthy et al. [22] reported activations of PCC in their auditory and visual oddball paradigms, respectively. Stevens et al. [31] reported activation of the PCC in their auditory task, but not in their visual oddball paradigm suggesting that the engagement of PCC may be modality-dependent. In contrast to these studies, a study of the auditory oddball task using single photon emission computed tomography (SPECT) reported that the 'posterior cingulate cortex appears to be inhibited during the oddball tasks' [12]. In the present study, we observed a clear activation focus on the PCC (Fig. 3c). Thus, our findings support those of McCarthy et al. [22], suggesting engagement of PCC during the performance of the visual oddball task.

In this study, we were able to reproduce the occipitotemporal activations reported by Clark et al. [7] and Yoshiura et al. [34] in their visual, but not auditory experiments. The results in Refs. [7,34], as well as those reported herein,
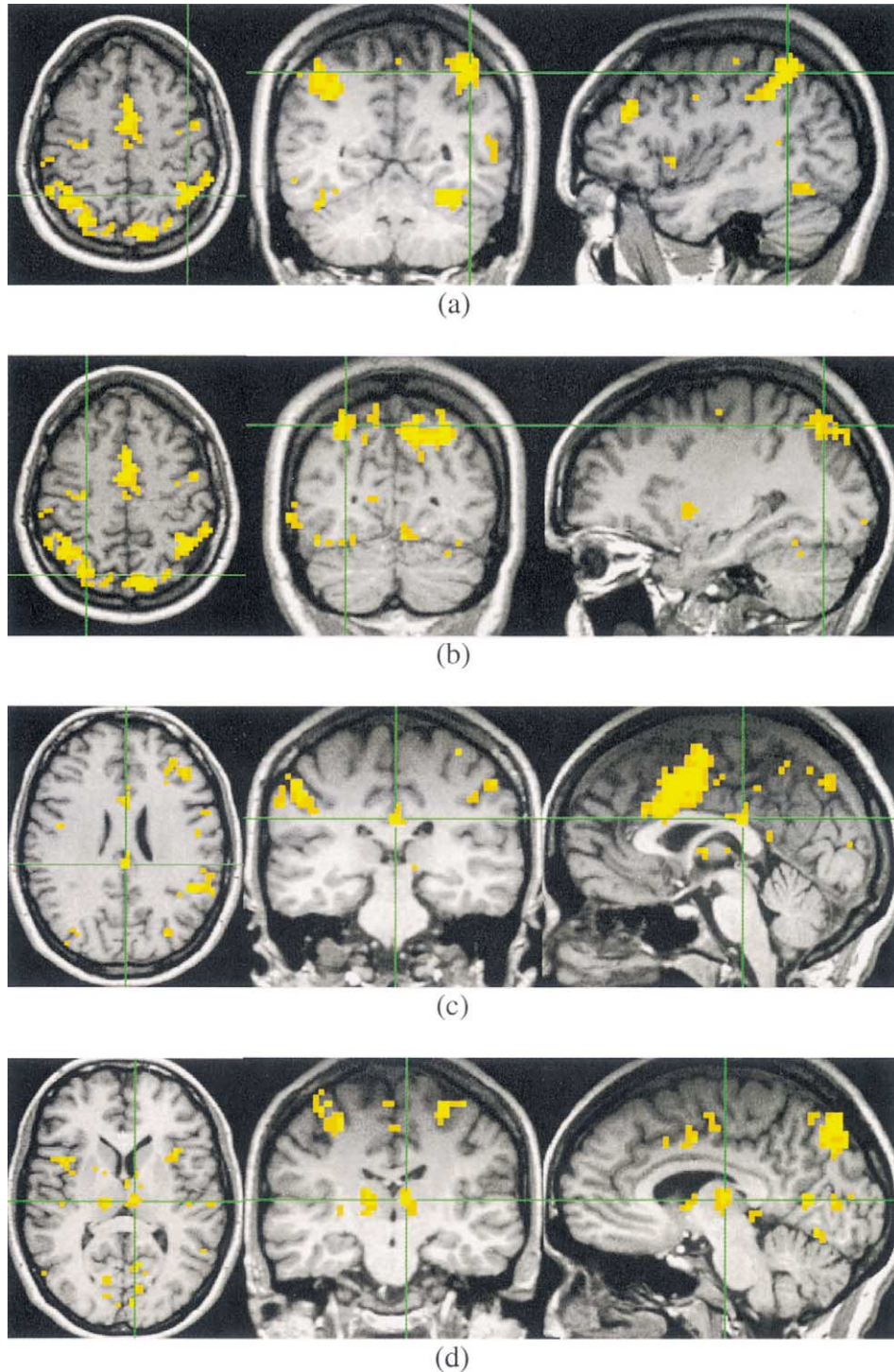
Fig. 3. Brain regions activated by the visual oddball paradigm: (a) inferior parietal lobule (supramarginal gyrus; BA 40), (b) superior parietal lobule (BA 7), (c) the posterior cingulate gyrus, (d) thalamus, (e) inferior occipitotemporal cortex (BA 19/37), (f) insula, (g) middle frontal gyrus (DLPFC), (h) anterior cingulate gyrus and medial frontal gyrus (BA 6), (i) premotor area (BA 6), and (j) cuneus (BA 17). All activations were bilateral. The color scale reflects the value of the statistic s (see Eq. (1) in the text) normalized to a maximum of 1 across the image. The activated regions are derived from EPI data of all seven subjects. However, the regions are superimposed on the MP-RAGE image of one of the subjects after registration to the Talairach–Tourneaux stereotactic atlas.

suggest the activation of the inferior occipitotemporal cortex to be modality-dependent, and most likely associated with the processing of object shape information in the visual oddball experiments [19,25]. A note of caution with respect to localizing activation in occipitotemporal lobe is that, when using the Talairach coordinates to localize brain
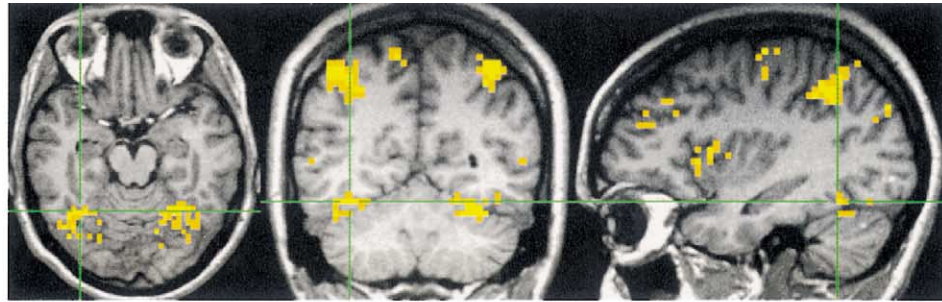
(e)
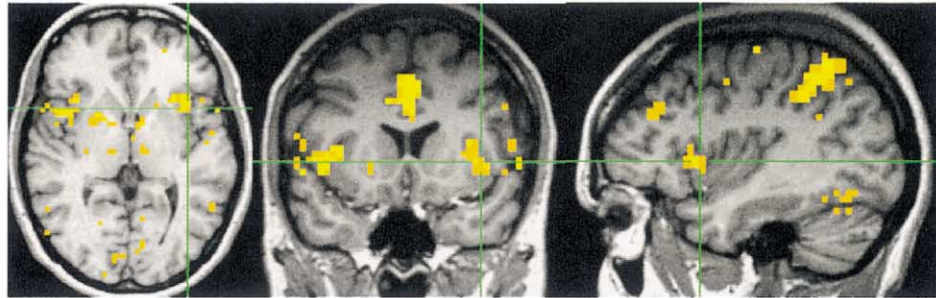
(f)
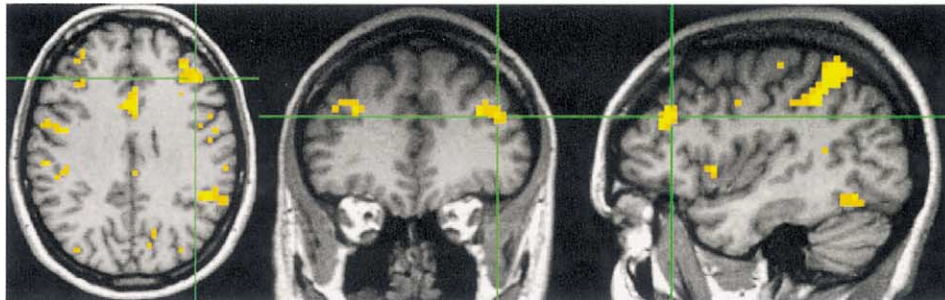
(g)
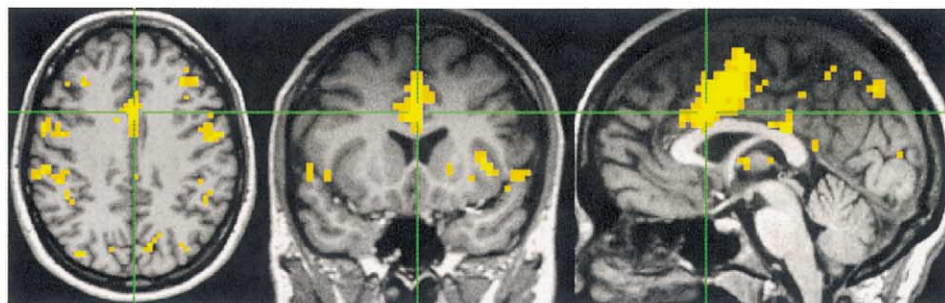
(h)

Fig. 3. (*continued*)

activity, the variability across subjects in the position of the cerebellum with respect to the cerebrum could falsely attribute activation of extrastriate visual cortex to cerebellum or vice versa.

Activation of primary visual cortex (BA 17; cuneus) (Fig. 3j) has been observed in many prior studies involving visual stimulation compared to rest. Our study, which involved contrasting infrequent target to more frequent standard events that were perceptually similar, suggests that this region may be engaged by cognitive processes relevant to registration of the targets. Activation in the superior (Fig. 3b) and inferior parietal lobule (Fig. 3a) has often been observed in paradigms that involve classification of visual stimuli. The bilateral activation in the
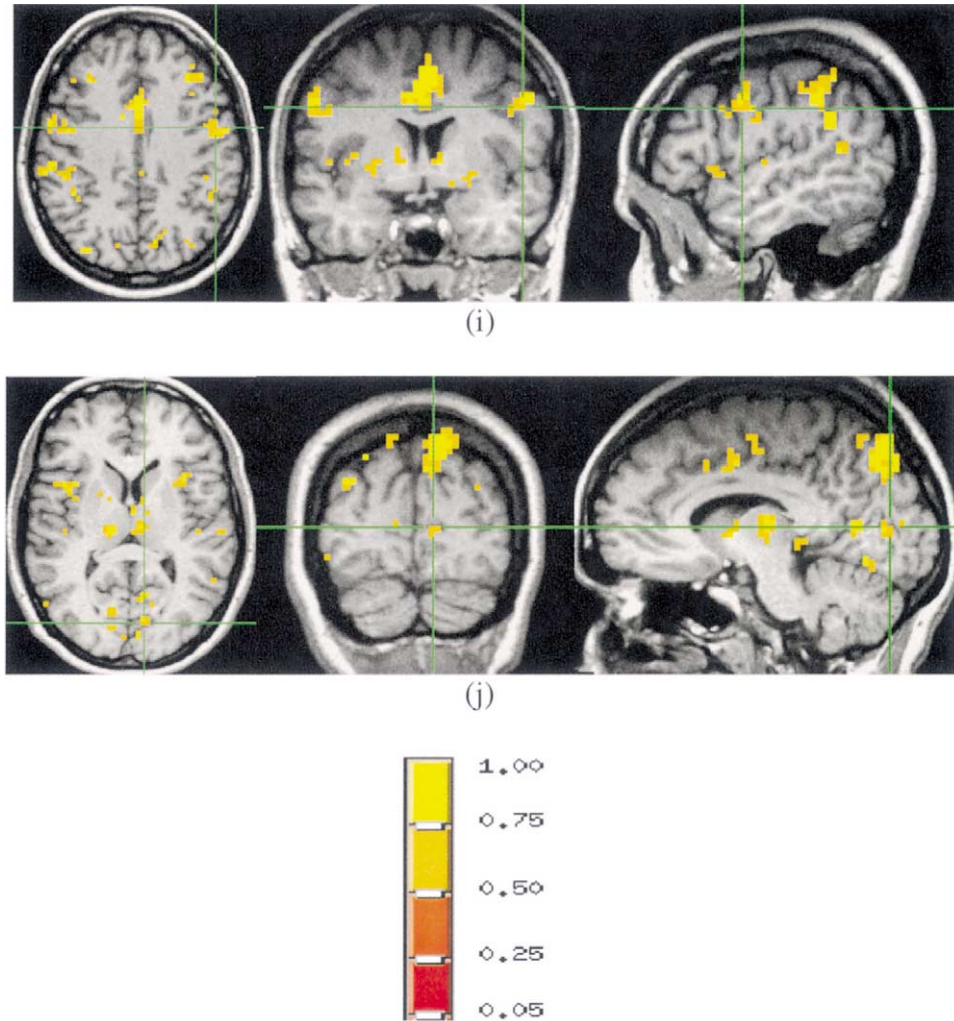
Fig. 3. (*continued*)
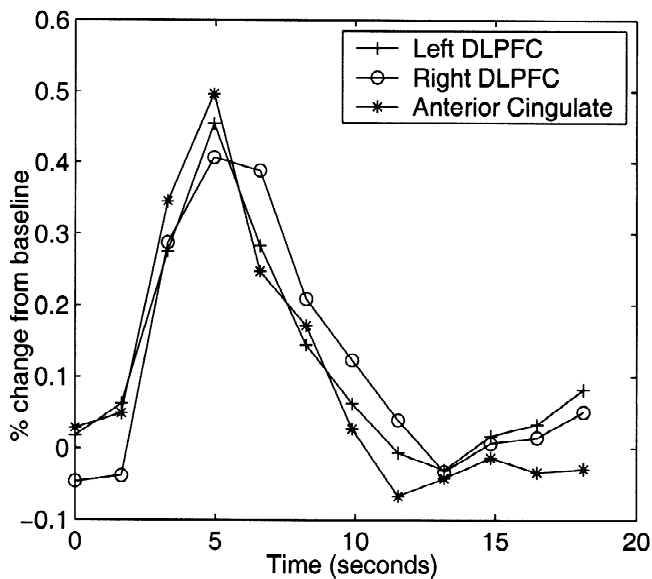
Fig. 4. The average (across voxels and target events) of the evoked stimulus responses for the left and right DLPFC and the anterior cingulate computed from the median data set.

premotor (Fig. 3i) and supplementary motor areas (Fig. 3c) has been reported in other studies that also required subjects to keep a silent count of rare targets without an overt motor response [31,34]. It has been proposed that these activations may be attributable to planning of an unexecuted motor orienting response or may represent a possible attentional role in sensory processing [11].

In conclusion, a non-parametric statistical analysis method that controls for multiple comparisons, requires no assumptions about the noise structure of the data, and applies no additional smoothing (except for the unavoidable smoothing incurred with spatial normalization and inter-subject data fusion) was applied to the analysis of near full-brain fMRI data obtained in a visual oddball paradigm. Most of the regions found activated in the present study have been implicated in the performance of working memory and selective attention tasks. The ACC and the bilateral SMG were found to be activated. These findings are consistent with the majority of the previously reported fMRI analyses of the oddball task. The findings of

this paper also provide additional evidence for the bilateral involvement of the DLPFC, insula, thalamus, premotor area, and the inferior occipitotemporal cortex.

Acknowledgements

References

[1] B.A. Ardekani, A.H. Bachman, J.A. Helpern, A quantitative comparison of motion detection algorithms in fMRI, Magn. Reson. Imaging 19 (2001) 959–963.

[2] J.R. Augustine, Circuitry and functional aspects of the insular lobe in primates including humans, Brain Res. Rev. 22 (1996) 229–244.

[3] M. Belmonte, D. Yurgelun-Todd, Permutation testing made practical for magnetic resonance image analysis, IEEE Trans. Med. Imaging 20 (2001) 243–248.

[4] R.C. Blair, W. Karniski, Distribution-free statistical analyses of surface and volumetric maps, in: R.W. Thatcher, M. Hallett, T. Zeffiro, E.R. John, M. Huerta (Eds.), Functional Neuroimaging: Technical Foundations, Academic Press, San Diego, CA, 1994, pp. 19–28.

[5] M.J. Brammer, E.T. Bullmore, A. Simmons, S.C.R. Williams, P.M. Grasby, R.J. Howard, P.W.R. Woodruff, S. Rabe-Hesketh, Generic brain activation mapping in functional magnetic resonance imaging: a nonparametric approach, Magn. Reson. Imaging 15 (1997) 763–770.

[6] E. Bullmore, C. Long, J. Suckling, J. Fadili, G. Calvert, F. Zelaya, T.A. Carpenter, M. Brammer, Colored noise and computational inference in neurophysiological (fMRI) time-series analysis: resampling methods in time and wavelet domain, Hum. Brain Mapp. 12 (2001) 61–78.

[7] V.P. Clark, S. Fannon, S. Lai, R. Benson, L. Bauer, Responses to rare visual target and distractor stimuli using event-related fMRI, J. Neurophysiol. 83 (2000) 3133–3139.

[8] M. Corbetta, F.M. Miezin, S. Dobmeyer, G.L. Shulman, S.E. Petersen, Selective and divided attention during visual discriminations of shape, color, and speed: functional anatomy by positron emission tomography, J. Neurosci. 11 (1991) 2383–2402.

[9] R.W. Cox, AFNI: software for analysis and visualization of functional magnetic resonance neuroimages, Comput. Biomed. Res. 29 (1996) 162–173.

[11] J. Downar, A.P. Crawley, D.J. Mikulis, K.D. Davis, A multimodal cortical network for the detection of changes in the sensory environment, Nat. Neurosci. 3 (2000) 277–283.

[12] K.P. Ebmeier, J.D. Steele, D.M. MacKenzie, R.E. O'Carroll, R.R. Kydd, M.F. Glabus, D.H. Blackwood, M.D. Rugg, G.M. Goodwin, Cognitive brain potentials and regional cerebral blood flow equivalents during two- and three-sound auditory 'oddball tasks', Electroencephalogr. Clin. Neurophysiol. 6 (1995) 434–443.

[13] J.M. Ford, A. Pfefferbaum, W. Roth, P3 and schizophrenia, Ann. NY Acad. Sci. 658 (1992) 146–162.

[14] K.J. Friston, A.P. Holmes, K.J. Worsley, J.P. Poline, C.D. Frith, R.S.J. Frackowiak, Statistical parametric maps in functional imag-

ing: a general linear approach, Hum. Brain Mapp. 2 (1995) 189–210.

[15] J. Green, A.I. Levey, Event-related potential changes in groups at increased risk for Alzheimer disease, Arch. Neurol. 56 (1999) 1398–1403.

[16] A.P. Holmes, R.C. Blair, J.D. Watson, I. Ford, Nonparametric analysis of statistic images from functional mapping experiments, J. Cereb. Blood Flow Metab. 16 (1996) 7–22.

[17] K.A. Kiehl, P.F. Liddle, An event-related functional magnetic resonance imaging study of an auditory oddball task in schizophrenia, Schizophr. Res. 48 (2001) 159–171.

[18] K.H. Knuth, B.A. Ardekani, J.A. Helpern, Bayesian estimation of a parameterized hemodynamic response function in an event-related fMRI experiment, Proc. Int. Soc. Magn. Reson. Med. 9 (2001) 1732.

[19] M. Kraut, J. Hart Jr, B.J. Soher, B. Gordon, Object shape processing in the visual system evaluated using functional MRI, Neurology 48 (1997) 1416–1420.

[20] D.E.J. Linden, D. Prvulovic, E. Formisano, M. Völlinger, F.E. Zanella, R. Goebel, T. Dierks, The functional neuroanatomy of target detection: an fMRI study of visual and auditory oddball tasks, Cereb. Cortex 9 (1999) 815–823.

[21] J.J. Locascio, P.J. Jennings, C.I. Moore, S. Corkin, Time series analysis in the time domain and resampling methods for studies of functional magnetic resonance brain imaging, Hum. Brain Mapp. 5 (1997) 168–193.

[22] G. McCarthy, M. Luby, J. Gore, P. Goldman-Rakic, Infrequent events transiently activate human prefrontal and parietal cortex as measured by functional MRI, J. Neurophysiol. 77 (1997) 1630–1634.

[23] V. Menon, J.M. Ford, K.O. Lim, G.H. Glover, A. Pfefferbaum, Combined event-related fMRI and EEG evidence for temporal-parietal cortex activation during target detection, Neuroreport 8 (1997) 3029–3037.

[24] P.L. Nunez, Electric Fields of the Brain: The Neurophysics of EEG, Oxford University Press, 2002.

[25] H. Op de Beeck, E. Beatse, J. Wagemans, S. Sunaert, P. Van Hecke, The representation of shape in the context of visual object categorization tasks, Neuroimage 12 (2000) 28–40.

[26] B. Opitz, A. Mecklinger, A.D. Friederici, D.Y. von Cramon, The functional neuroanatomy of novelty processing: integrating ERP and fMRI results, Cereb. Cortex 9 (1999) 379–391.

[27] E. Paulesu, C.D. Frith, R.S.J. Frackowiak, The neural correlates of the verbal component of working memory, Nature 362 (1993) 342–345.

[28] J. Polich J, A. Kok, Cognitive and biological determinants of P300: an integrative review, Biol. Psychol. 41 (1995) 103–146.

[29] B. Porjesz, H. Begleiter, Neurophysiological factors in individuals at risk for alcoholism, Recent Dev. Alcohol. 9 (1991) 53–67.

[30] T. Shinba, Y. Andow, T. Shinozaki, N. Ozawa, K. Yamamoto, Event-related potentials in the dorsal hippocampus of rats during an auditory discrimination paradigm, Electroencephalogr. Clin. Neurophysiol. 100 (1996) 563–568.

[31] A.A. Stevens, P. Skudlarski, J.C. Gatenby, J.C. Gore, Event-related fMRI of auditory and visual oddball tasks, Magn. Reson. Imaging 18 (2000) 495–502.

[32] S. Sutton, M. Braren, J. Zubin, E.R. John, Evoked potential correlates of stimulus uncertainty, Science 150 (1965) 1187–1188.

[33] J. Talairach, P. Tournoux, Co-Planar Stereotaxic Atlas of the Human Brain, Georg Thieme Verlag, New York, 1988.

[34] T. Yoshiura, J. Zhong, D.K. Shibata, W.E. Kwok, D.A. Shrier, Y. Numaguchi, Functional MRI study of auditory and visual oddball tasks, Neuroreport 10 (1999) 1683–1688.